Thyroxine incorporated commercially available alginate dressings to stimulate angiogenesis for wound healing applications

Graphical Abstract:

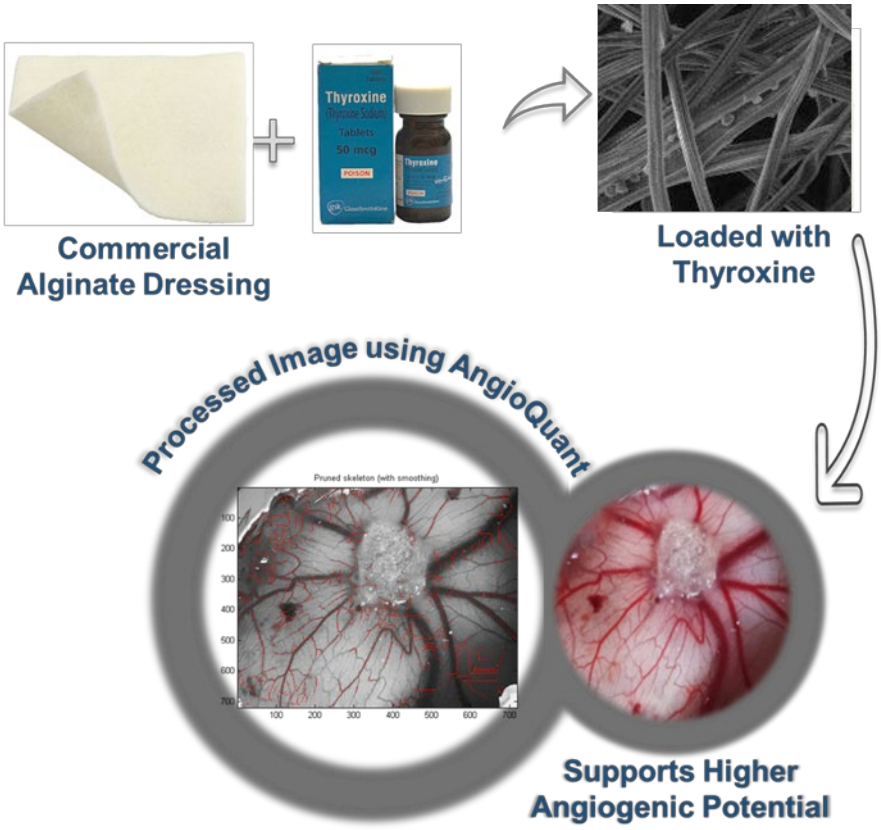

Thyroxine incorporated commercially available alginate dressings to stimulate angiogenesis for wound healing applications

Rida Badar[a], Saima Zulfiqar[a], Alap Ali Zahid[a], Nadia Mehmood[a], Rabia Zeeshan[a], Ayesha Nawaz[a], Najiya al-Arifa[b], Anwarul Hasan[c,d], Sher Zaman Safi[a], Ihtesham ur Rehman[e], Muhammad Yar[a,*]

[a]*Interdisciplinary Research Center in Biomedical Materials, COMSATS University Islamabad Lahore Campus, Lahore, 54000, Pakistan*

[b]*Department of Zoology, Lahore College for Women University, Lahore, Pakistan*

(Najiya.alArifa@LCWU.edu.pk)

[c]*Department of Mechanical and Industrial Engineering, College of Engineering, Qatar University, Doha, Qatar*

[d]*Biomedical Research Center, Qatar University, Doha, Qatar*

[e]*School of Medicine, University of Central Lancashire, Preston, Lancashire PR1 2HE UK*

For Correspondence:

[*]*Interdisciplinary Research Center in Biomedical Materials, COMSATS University Islamabad, Lahore*, Campus, *54000, Pakistan*; Tel: 0092 42 001007 extension 828; Fax: 0092 42 35321090

E-mail: drmyar@cuilahore.edu.pk (M. Yar)

Abstract

Advanced wound care products had attracted great attention and particularly materials stimulating angiogenesis is one of the major focussed area. The identification of suitable angiogenic agents and then delivery from a well accepted carrier materials, ideally the one being already in clinical use is well adopted approach. Alginate dressings are very well accepted dressings worldwide in clinic and in present work alginate dressings were modified to support angiogenesis by loading thyroxine. To study the affect of concentration of thyroxine, 1 µg/ml, 5 µg/ml and 10 µg/ml thyroxine was loaded into alginate dressings. Any chemical changes in the dressings after loading thyroxine was studied by FTIR analyses and it was found that loading of thyroxine did not produce any chemical change in alginate dressings. The sustained thyroxine release upto 74% was observed in the phosphate buffer pH 7.4 over seven days time. The cytotoxicity study was conducted using fibroblasts cells and all thyroxine concentrations were found to be biocompatible and assisted cells proliferation. Real time PCR was used to evaluate the gene expression of fibroblasts treated with synthesized alginate hydrogels to evaluate the effect of thyroxine on genes involves in angiogenic pathway. To study angiogenic activity chorioallantoic membrane (CAM) assay was performed, it was observed higher number of new junctions, angiogenic potential was shown by 5 µg/ml thyroxine loaded alginate dressings. These results suggested that the thyroxine loaded alginate dressings have very high potential of fast wound healing.

Keywords: Thyroxine, Alginate, CAM assay, Angiogenesis, Tissue engineering, Wound healing, FTIR, Gene expression, Biocompatible, Fibroblas cells

1 Introduction

In human body, skin tissue is the largest, most exposed, and also most vulnerable tissue [1, 2]. Once the damage of skin tissue occurs, the repair process appears to be very complex, [3-5] which includes four interactive and classic phases: hemostasis, inflammation, proliferation, and remodeling/maturation [6]. Although most skin defect can be quickly and effectively healed within 1 or 2 weeks, [7, 8] the extensive full-thickness wounds are often hard to repair, which presents serious impact on health and even threaten people's life [9]. Therefore, a variety of biomaterials have been developed as wound dressings, such as nanofibers, sponge, foam, and hydrogels [10, 11] among them, alginate is an acidic linear polysaccharide composed of guluronic acid and mannuronic acid moieties in variable proportions, which is widely used in the industry and

medicines for many applications such as scaffolds and wound dressings [12, 13]. In particular, it is able to form stable aqueous hydrogel by physically crosslinking with multivalent cations such as calcium (Ca^{2+}) [14]. Until now, there are several forms of alginate-based wound dressings, including hydrogel, film, nanofiber, foam and sponge, etc. [15]. Among them, the sponge-like dressings are most attractive because in addition to the outstanding biocompatibility and biodegradability, they are able to absorb excess wound exudate while maintaining a moist wound environment [16, 17] due to their porous structures, which can be accurately controlled by the concentrations of the alginate solution and crosslinkers [18, 19]. Moreover, this controllable porous structure makes the alginate spongy matrix a good delivery system for bioactive substances to enhance wound healing. Alginate dressings such as Algosteril, Algisite, Sorbsan, Algisite M, SeaSorb, Melgisorb, Sorbalgon, Kaltostat, Curasorb, and Tegagen T are commercially available and being used in clinics for healing of various types of wounds.

Wound healing, a fully organized process, undergoes four phases: hemostasis, inflammation, proliferation, and remodeling, while the inflammation phase is prolonged in diabetic wounds, assuming slow or stall wound healing [20-22]. After an injury, platelets are activated leading towards the formation of a thrombus (hemostasis). Then, during an inflammation phase, mast cells release neutrophils and M1 macrophages that clear away bacteria and damaged tissue from the wound. The proliferative phase initiates when macrophages modify into an anti-inflammatory M2 phenotype. Here, cells extrude healing factors that stimulate the differentiation of stromal cell proliferation, neovascularization and angiogenesis, and the formation of granulated tissue [23, 24]. During the remodeling phase, reorientation of matrix and cells takes place, as a result, normal cells are formed [25]. Pathophysiologic alterations associated with diabetic wound healing are increasingly understood to result from both systemic impacts of diabetes and intrinsic alterations in the cells responsible for regenerating damaged tissue.

Thyroxine (T4) is a hormone that is secreted by thyroid hormone. It controls various physiological functions in the body for proper growth [26]. Concerning it, there are some reports published, which confirmed its angiogenic potential. Chilian and Tomanek proposed neovascularization together with tissue growth due to thyroxine [27-30]. In 2004, Paul J. Davis and co-workers investigated thyroxine ability to enhance blood vessels formation up to three folds as compared to control [31]. The preparation of porous biodegradable membranes loaded with thyroxin could

prove to be a promising material for skin regeneration related issues. Considering these aspects, thyroxine, stimulates angiogenesis via distinctive mechanisms [32]. Mainly, thyroxine leads to transcription of basic fibroblast growth factor (bFGF) as well as vascular endothelial growth factor (VEGF), responsible for blood vessel growth by triggering integrin αvβ3 [33]. Prevously, our group investigated the pro-angiogenic potential of thyroxine (1 µg and 10 µg/mL) loaded chitosan hydrogels by chick chorioallantoic membrane assay; that conferred 1 µg loaded thyroxine hydrogel the best fit, due to the formation of blood vessels with and within scaffold [[34].

We aimed to prepare thyroxine loaded clinically used alginate dressings with different concentrations of thyroxine (1µg, 5µg, 10µg). The release profile of thyroxine and antibacterial studies on synthesized hydrogels were carried out. The CAM assay, a very effective bioassay to evaluate the angiogenic potential of material, was used in this study to investigate the angiogenic potential of synthesized materials. Cell cytotoxicity studies were conducted to confirm the biocompatibility, non-toxic and non-immunogenic nature of materials. These dressing materials were also studied for their ability to stimulate the genes (VEGF, IL-10, IL-1β and cPGE) responsible for angiogenesis and wound healing. Alginates were proved to be the appropriate dressings to encapsulate thyroxine for potential application to stimulate blood vessel formation to accelerate wound healing.

2 Materials and methods

Phosphate buffer saline (PBS) was purchased from Sigma-Aldrich, USA. Commercially available alginate dressings were procured from Advanced Medical Solutions. Thyroxine (**SC-207813A Santa Cruz, California**) was purchased from GlaxoSmithKline (GSK, Pakistan). These were all standard chemicals, used without any further purification.

2.1 FTIR (Fourier Transform Infrared spectroscopy)

Chemical structures of thyroxine loaded alginate dressings and simple alginate dressings were determined by FTIR spectroscopy, (Thermo Nicolet 6700P, USA). ATR mode was used to record spectra at room temperature with $8cm^{-1}$ resolution and 256 scans between 4000 and $650cm^{-1}$.

2.2 Loading of thyroxine into alginate dressings

Alginate dressings were encapsulated with thyroxine in an aseptic environment. For this purpose, 60mm patches of pre-sterilized alginate dressings were pruned and solutions of thyroxine in

distilled water with different concentrations such as 1 µg/ml, 5 µg/ml and 10 µg/ml were filtered. These were loaded onto dressings under a sterile environment in a biosafety cabinet and then dressings were dried at room temperature. The final products were thyroxine loaded alginate and named as 1TA (1 µg/ml), 5TA (5 µg/ml), and 10TA (10 µg/ml).

2.3 SEM Analysis

The surface morphology of the synthesized e-spun mats was examined by using a scanning electron microscope (TESCAN, VEGA LMU, Czech Republic). The images were taken at different magnifications. The pore size and fiber diameter were calculated by measurement of randomly selected 10 fibers using open-source image-processing software Image J.

2.4 Thyroxine loading estimation

To estimate thyroxine drug in alginate dressings, stock solution and dilutions of thyroxine in PBS were prepared. Then, absorption spectra of all dilution were recorded in the wavelength range 200nm to 800nm in the UV-VIS spectrophotometer (PerkinElmer Lambda 25, USA). The values of absorption of all dilutions were taken, and a calibration curve was drawn. And finally, the concentration of released drugs from the alginate dressings was deduced from the calibration curve.

2.5 Drug release studies

For the release of thyroxine, the methods adopted by Shazadi et al. was used [35]. Dressings, filled with thyroxine, of the same size (103 mg) were immersed in PBS at physiologic temperature. All solutions absorption values were assessed at the wavelength of 227nm by UV visible spectrophotometer after a specific time interval. The maximum thyroxine release was determined for one week. *In vitro* drug release was executed by having thyroxine-alginate dressings (~0.1 g) in 4 ml of phosphate buffer pH 7.4 at 37 °C. At definite period, all the time has withdrawn volume of PBS was replaced with fresh dissolution medium to manage consistent thyroxine release. Thyroxine release was confirmed via a UV/Vis spectrophotometer at λ_{max} 227 nm. The experiments were performed in triplicates.

2.6 Swelling studies

The swelling behavior of dressings was investigated using the gravimetric technique. The degree of swelling of alginate dressings was investigated in PBS (phosphate buffer saline) solution pH

7.4 at 37°C. Absorption rates were recorded by removing the swollen samples at a predetermined time. Following time intervals were followed i.e., 30 mins, 2hrs, 4hrs and 16hrs. There was a notable difference in dry weight and wet weight of dressings. All measurements were performed in triplicates. The swelling index was calculated by the following formula.

$$\text{Swelling\%} = W\text{-}W_d / W_d * 100$$

2.7 *In vitro* cytotoxicity assay

In vitro cytotoxicity study of commercially available alginate dressings modified with thyroxine impregnation, was conducted using Alamar Blue assay. For this, extracts of the samples were prepared in a cell culture medium according to recommendations of ISO 10993-12. Hence, all sample disks (8mm) were soaked in cell culture medium (Dulbecco's Modified Eagle Medium (DMEM), supplemented with 10% (v/v) fetal bovine serum (FBS), and 1.0% penicillin-streptomycin for 48 hrs, in 24 well plate. Then, these were centrifuged at 1000rpm and the supernatant was separated and preserved at 4°C for further use. The sterility of these extracts was tested by contamination testing by incubating an aliquot of each sample in an incubator for 24 hrs. The indigenous extracts were diluted in 1:1 in cell medium. The murine fibroblast cells (NIH/3T3) 1×10^4 cells /mL were cultured for 24 hrs and treated with the extracts dilution and incubated in humidified 5% CO_2 at 37°C for 1, 5, and 7 days. The addition of Alamar Blue solution (100µl) and 4 hrs incubation was followed by measuring absorbance at 570nm after 4 hrs. The analysis was performed in triplicate.

2.8 RNA Extraction and Gene Expression Analysis

The cellular lysate was used to extract total RNA by using an RNA extraction kit (Ko721 Thermo, USA) according to the instructions of the manufacturer. For the synthesis of cDNA through reverse transcription, while using 1 µg total RNA for each sample along-with random hexamers by SuperScript III Supermix (Invitrogen, US) in 20 µL final reaction volume.

For real time PCR, cDNA (1µl) was added to Sybergreen Fast Universal PCR Master Mix as well as Sybergreen Gene Expression Assay primer/probe mixes (Applied Biosystems, Foster City, US) to get a final reaction volume of 20 µL. Applied Biosystems 7900HT Fast Real-Time PCR System was used to execute RT-PCR. C_T data were collected via Sequence Detection Systems 2.3 software (Applied Biosystems). The experiment for each cell sample was performed twice against one gene.

To calculate the fold change in target gene expression, β-actin was used as control, and the following formula was used:

$$\Delta\Delta Ct = (Ct_{target}\text{-}Ct_{\beta\text{-}actin})_{treated} - (Ct_{target}\text{-}Ct_{\beta\text{-}actin})_{control}$$

2.9 Scratch wound assay:

The migration of fibroblasts NIH-3T3 was evaluated by scratch wound assay, which expresses the migration of cells on the surface of the thyroxine loaded clinically used alginate dressings. For this, 3×10^4 cells/ml were seeded in 6 well plates experiment was performed at 80% confluency. Then, a linear scratch was created in the cell monolayer with a sterile 100 µl pipette tip and these dressings were placed at a side of the wound. Then, the 6 well plates (Corning Inc., USA) were placed in an incubator at 37 °C and 5% CO_2. After 24 hrs, images were captured under VWR inverted fluorescence microscope.

2.10 CAM assay

The angiogenic potential of alginate dressings was assessed by CAM assay [36, 37]. Such role of thyroxine loaded alginate dressings was evaluated. On the 6th day, fertilized eggs were purchased from the Big Bird Group (Lahore, Pakistan). After rinsing with 20% ethanol, these were incubated at 37 °C with 55% humidity. On the 7th day, a square hole (1 cm^2) was made onto the eggshell and samples were placed onto CAM followed by sealing with cellophane tape and incubated at 37 °C with 55% humidity. On day 14th, the camera images were taken while these alginate dressings were still on CAM and then were fixed in 10% paraformaldehyde for histological studies. The eggs were sacrificed on the same day.

2.11 Histology Studies

Control and thyroxine loaded alginate dressings sampled retrieved from the 14th day chick embryo of CAM assay were placed in 10% formaldehyde solution. Then these were used to evaluate the formation of blood vessels. For this, hematoxylin and eosin (H&E) stained embedded slices were analyzed under VWR inverted fluorescence microscope to mark the infiltration of blood vessels within CAM.

2.12 Statistical Analysis

All experiments were executed in triplicates and their results were calculated as mean ± S.D. The statistical analysis (unpaired Student's t-test) was performed via Graph-Pad QuickCalcs

(https://www.graphpad.com/quickcalcs/ttest1.cfm). All these results with a p value ≤0.05 were considered statistically significant.

3 Results and discussion

In this research study, micro and nanoporous commercial alginate dressings were used. The proangiogenic properties were augmented by thyroxine loading into the aldinate dressing. Various *in vitro* experiments were performed to investigate their potential as an effective material for the healing of full-thickness wounds.

We reported on the effects of loading thyroxine hormone to alginate dressings for regeneration of diabetic skin wounds. The fabrication of thyroxine loaded alginate dressings, their characterization and their potential use in angiogenesis have been represented in Fig. 1.

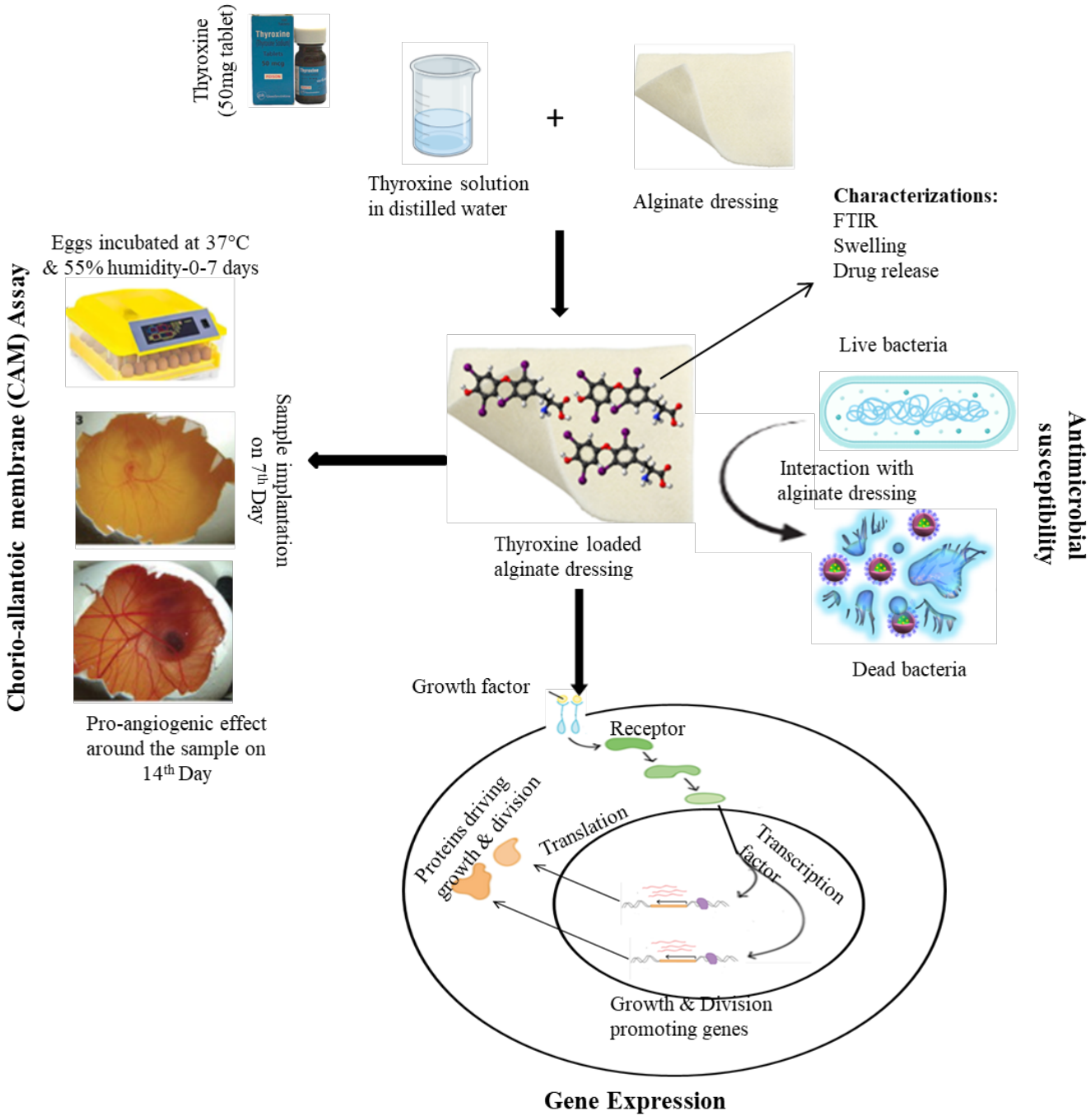

Figure 1: Schematic representation of fabrication of Thyroxine loaded alginate dressings, their antibacterial susceptibility, angiogenic potential, and gene expression

3.1 FTIR analysis

Fig. 1(A) and 1(B) represent FTIR spectra of alginate dressings, control without thyroxine and with thyroxine (1 µg/ml, 5 µg/ml and 10 µg/ml). The interaction of thyroxine with alginate was

confirmed by characteristic peaks of functional groups. The peak at 3400–3200 cm^{-1} exhibited O-H and N-H stretching vibration of alginate, evident in FTIR spectra of alginate dressings. Furthermore, a particular peak of amide I in alginate dressing appeared at 1655 cm-1 [38, 39]. The peak between 1630 cm^{-1} and 1650 cm^{-1} represented the carbonyl group of thyroxine.

3.2 SEM analysis

SEM analysis was performed to analyze the morphology of synthesized materials. Figure 2 (C) shows surface morphology of alginate dressings. The nanofibrous membranes dressings showed a porous fibrous structure with smooth surface morphology. After the incorporation of thyroxine, it was observed that fibre diameter was increased with increasing in the concentration of thyroxine. The mean porosity of the samples was estimated to be 26%, 39.41%, 51.782% and 69% for TA, 1TA, 5TA and 10TA, respectively, as depicted in figure 2(C). The average fiber diameter of TA was 0.5±0.3µm, 0.60±0.35 µm of 1TA, 0.765±0.142 µm of 5TA and 0.852±0.095 µm of 10TA, as shown in Fig. 2(D).

The loading of thyroxine into alginate dressings with various contents 1, 5 and 10 µg resulted in thyroxine aggregates on the surface. The number of these aggregates were increased as thyroxine content on the surface was increased. Thyroxine was in different agglomerations compared with smooth surface area and rough morphology, as in figure 2. The homogeneous, hydrophobic, or miscibility behavior of alginate fibres and thyroxine components could also be attributed to morphological differences. The introduction of high thyroxine explained this behavior, contributing to developing a high amorphous form and structural toughness. As a result, with increasing thyroxine concentration, resulted in rough surfaces due to the high thyroxine content.

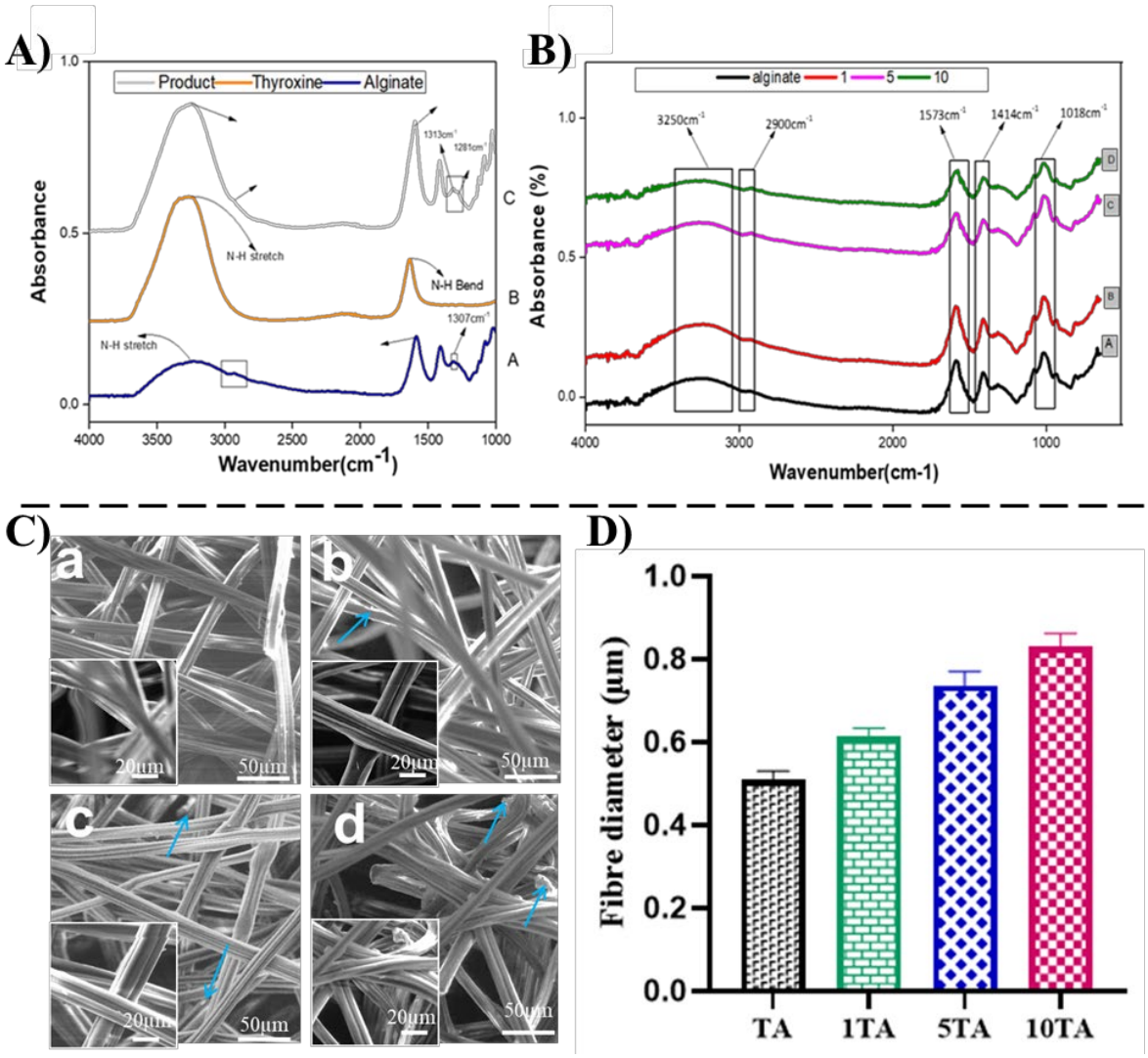

Figure 2: A) FTIR spectra of Alginate, Thyroxine and thyroxine loaded alginate membrane; (B) shows FTIR spectra of TA(Control),1TA, 5TA,10TA; C) SEM images of alginate dressing without thyroxine (a), and with thyroxine (b), (c) and (d) showing pore morphology with a scale bar of 20µm and 200 µm. D) Histogram showing average fiber diameter of these dressings.

3.3 Absorption studies

As alginate dressings retain a large amount of water, these can be used to absorb exudates from wounds. Instant exudate uptake is a crucial aspect for ideal wound dressings [38], so the fluid absorption capability of thyroxine loaded alginate dressings was traced. So, PBS, an isotonic and non-toxic with pH = 7.4, the most commonly used in *in-vitro* cellular level studies [39] was used. Fig. 3(A) exhibits time dependent swelling profile of alginate dressings with and without thyroxine. The 1TA exhibited a maximum swelling equilibrium while the control hydrogel showed minimum swelling equilibrium.

All dressings demonstrated a steady swelling ratio after 6 hrs. This property depends on thyroxine concentration. It was noticed that the swelling of dressings was decreased with the increase in the concentration of thyroxine significantly. This might be due to crosslinking, which altered the mobility of thyroxine within polymer chains, reduced the diffusion of PBS into the polymeric network, thereby producing a more rigid structure of the polymeric network [37].

Swelling studies indicates that drug has a significant effect on the integrity of dressing. When there was no drug, fibers of alginate disintegrated in PBS solution, but when thyroxine drug was added, the structure of fibers becomes compact and dressing did not break down in PBS solution, instead, it remained intact. Hence the % swelling of control (only alginate) decreases over time while the % swelling of 5TA dressings increases with time and drug concentration. There was a correlation between an increase in concentration and increase in %swelling.

3.4 Quantitative estimation of Thyroxine

Thyroxine released from loaded dressings was quantified via a UV-Visible spectrophotometer. Diluted solutions of thyroxine were prepared in a range of concentrations (i.e. 0.125, 0.25, 0.375, 0.5, 0.625, 0.75, 0.875 and 1 μg/mL) and their absorbances taken at 227 nm were used to plot a calibration curve. Then, thyroxine loaded alginate dressing of equal weights was immersed in PBS solution to investigate the release of thyroxine at different periods. The absorbance value of released media was determined through a spectrophotometer and thyroxine concentration was deduced from the calibration curve.

To use these dressings for drug delivery or as implants, *in vitro* drug release was investigated at pH 7.4.

Less drug release was observed from batch 1TA, 5TA, and 10TA, with an increase in the concentration of thyroxine (fig. 3(B)) due to an increase in the concentration of citric acid and crosslinking density. Subsequently, decreased swelling ability and thyroxine release were observed.

10TA showed active drug release during 7 days, up to 74% as compared to other dressings, as depicted in Fig. 3(B). This release behavior showed active nature of dressings that they can deal with the wound effectively for 7 days with the thyroxine release and can retain the moisture at the injury site for 7 days.

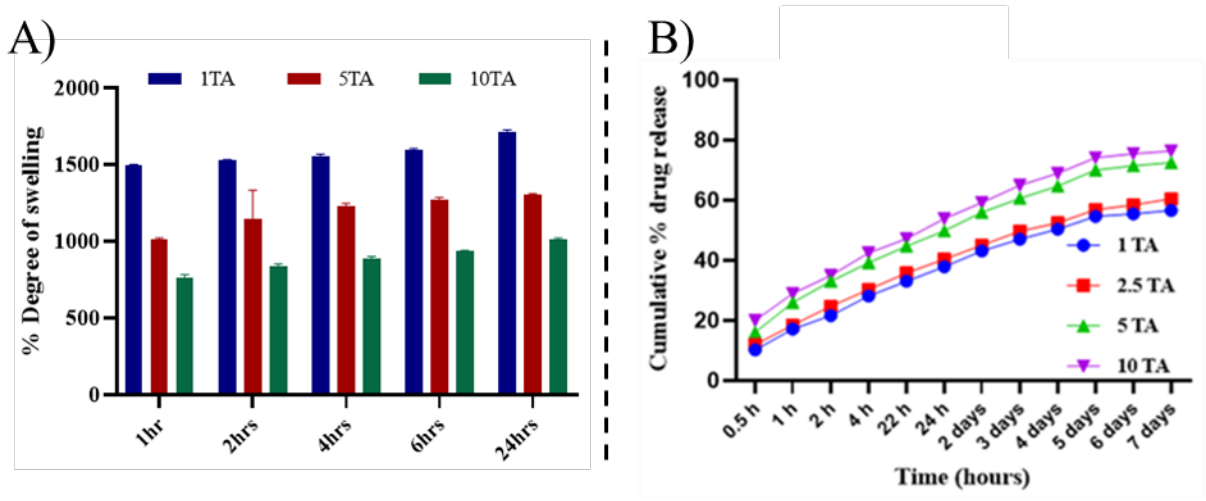

Figure 3: A) Swelling studies of thyroxine loaded alginate ~~hydrogels~~ dressings in PBS solution at 1, 2, 4, 6 and 24 hours; B) Release profile with calibration curve of thyroxine at different concentrations (0.125, 0.25, 0.375, 0.5, 0.625, 0.75, 0.875 and 1 µg/mL) from ~~the hydrogel~~ alginate dressings

3.5 In vitro Cytotoxicity assay

To evaluate the biocompatibility of thyroxine loaded commercially available dressings, Alamar blue assay was performed, as demonstrated in Fig. 4(A). The results of cell viability were compared with those of non-exposed cells (control). The results showed that these dressings were nontoxic towards fibroblasts. A linear manner was witnessed among all study groups at each time interval, while the increase in cell viability was noticed. There was an obvious difference between and within the groups (0.0001). This *in-vitro* cytotoxicity assay represented significant biocompatibility of the dressings. After 1, 5 and 7 days of incubation the fibroblast cells viability was observed between 102-107%, 111-147% and 149-165% respectively. This showed that healthy cell activity despite the release of thyroxine in the media, which does not have an anti-proliferative and cytotoxic effect towards fibroblasts. These studies exhibited that these dressings are highly biocompatible, non-toxic and non-immunogenic. So, the above-mentioned characteristics proved that these dressings have the potential to be used as dermal constructs without any harmful effects.

3.6 Gene expression analysis

Expression of VEGF was observed in 5TA, as compared to control, 1TA and 10TA. So, it was revealed that thyroxine up-regulated the expression of VEGF which in turn promoted angiogenesis. Guo et al [40] published the same results. In their study, they concluded that VEGF encourages angiogenesis which can be a key factor to treat ischemic diseases. From our results, it was also clear that our hydrogels increase the expression of VEGF and induces angiogenesis. We presumed that the receptor of the VEGF performs a similar role in the development of increased angiogenesis. It also stimulates extracellular matrix (ECM) probably through the linkage with VEGF and promotes angiogenesis, as shown in Figure 4(B). The IL-10 exhibited the same response, as shown in Figure 4(B). It acts as an anti-inflammatory cytokine the enhanced IL-10 expression not only plays a positive role in wound healing but also stimulates STAT3 transcription factor, through downstream signaling involving JAK-STAT and MAPK pathways. Inflammation is one of the protective mechanisms of the body in response to injuries and infections. However, at certain points, inflammation causes damage when it goes out of control. In many instances, it needs to be controlled through anti-inflammatory cytokines. One such example is IL-10 which limits the release of pro-inflammatory cytokines and chemokines and consequently prevents inflammation [41]. TNF-α also played an important role in stimulating the angiogenic potential. Lyer et al. reported that downregulation of IL-10 is associated with several autoimmune disorders and increased immunopathology [42]. Our results are in line with these studies, and we presume that its enhanced expression plays a positive role in angiogenesis and wound healing. As shown in Fig. 4(B), 5TA upregulates the expression of IL-1B probably via the MAK pathway involving VEGF-A and VEGFR signaling. It increases leukocyte penetration on the wound site that enhances proliferation, migration and angiogenesis in fibroblast cells.

Vascular endothelial growth factor (VEGF) is a very important contributor of new vessel formation during healing. This is an established fact and is demonstrated by a number of studies [43, 44]. In addition, VEGF acts as a proinflammatory cytokine by increasing endothelial cell permeability, by inducing the expression of endothelial cell adhesion molecules and other pro-inflammatory factors [45-49].

Just like VEGF, it has long been established that IL-1 is capable of simultaneously regulating inflammation and angiogenesis. Indeed, one of IL-1's earliest names was haemopoeitn-1 due to its

pro-angiogenic effects [50, 51]. Looking at our results, it clearly show up-regulation of VEGF and IL-1 beta which demonstrate that the pro-angiogenic effect might be taking place through VEGF and IL-1β. Studies have revealed various overlaps in several pathways such as mitogen activated protein kinase (MAPK) which is induced by IL-1 beta and VEGF and thus may potentially play a role in the overlapping effects caused by inflammatory and angiogenic signaling [52]. Having said that, the cells must retaliate to the proinflammatory factors (VEGF and IL-1β) in the form of anti-inflammatory factor. The IL-10 is a known anti-inflammatory cytokines and the increased level of IL-10 might be due to the increased inflammation that caused by the pro-inflammatory factors as discussed above.

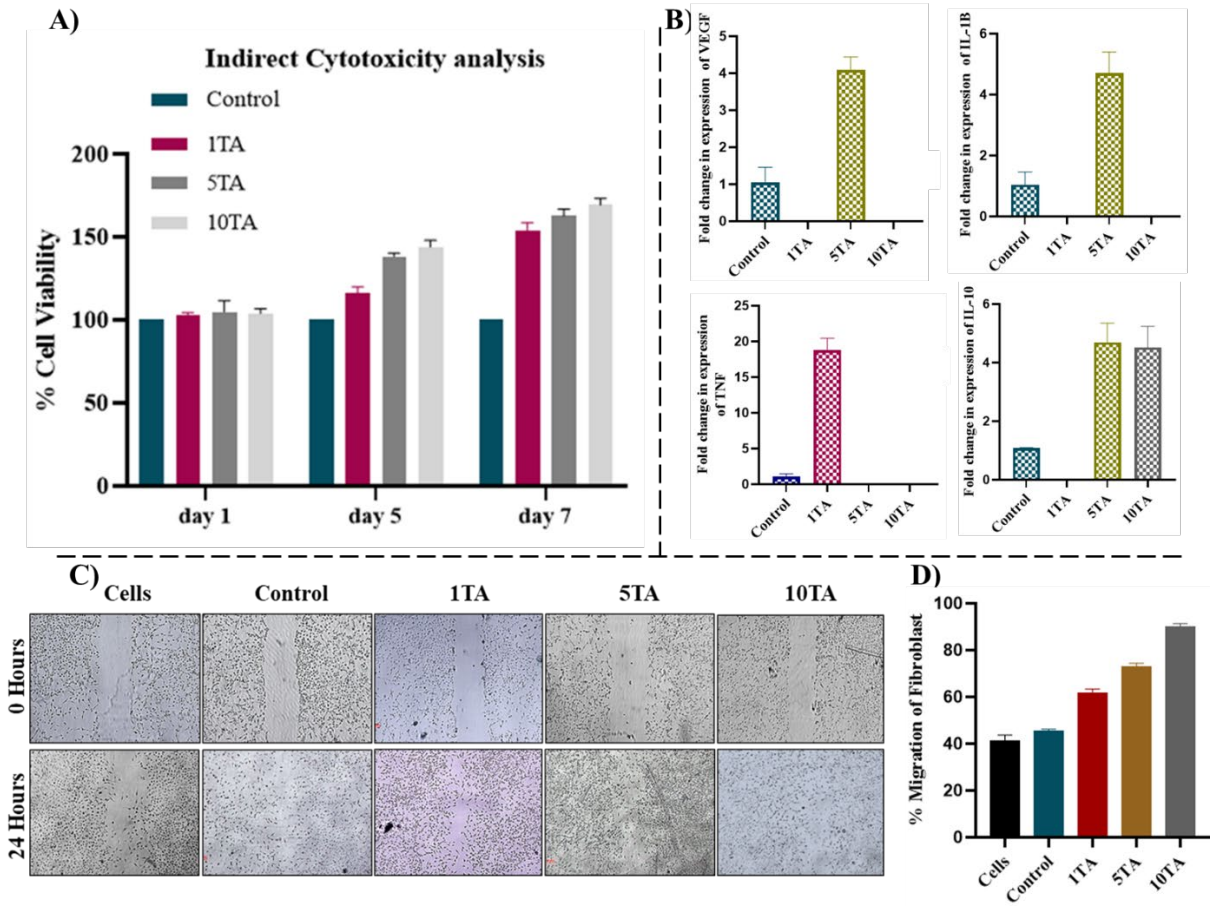

Figure 4: A) Cell viability of the thyroxine-loaded alginate dressings by Alamar Blue assay for *in vitro* cell proliferation ($p < 0.0001$). Cell viability analysis on Fibroblasts (NIH-3T3) cells treatment to control, 1TA, 5TA, and 10TA at wavelengths of 570 nm. Note that the absorbance values increase significantly from day 1 to day 7: B) Expression of VEGF, IL-10, IL-1B and TNF-

α in different dressings; C) Fibroblast (NIH-3T3) cells were cultured for 48 hours. After straight-line scratching, cells were subjected to control, 1TA, 5TA and 10TA respectively for 24hours; D) Percentage of wound healing was measured and presented on a histogram using ImageJ software. ($P < 0.001$).

3.7 Wound healing Scratch Assay

As migration of cells is the most important phase of the healing process, time dependent cell migration behavior of fibroblasts NIH-3T3 was performed for 0-24 hours in the presence of alginate dressings with distinct concentrations of thyroxine. The qualitative results have been shown in Fig. 4. We proposed to study any harmful effect of these dressings on the morphology and growth of fibroblast NIH-3T3 cells. The results exhibited relatively faster migration of fibroblasts in dressings having thyroxine (1TA, 5TA & 10TA) as compared to control. We observed that 10TA showed almost 100% migration of cells. It was concluded that these dressings provided a non-toxic environment helping in the growth and proliferation of the cells. The overall results (Fig. 4(C)) indicated the pre-antigenic property of 5TA and 10TA dressings.

3.8 Evaluation of angiogenesis by CAM assay

Thyroxine loaded alginate dressings were successfully prepared and tested for their angiogenic activity by *in-ovo* CAM assay. Fig. 5(A) and 5(B) show the results of the thyroxine loaded alginate dressings on the CAM on the 14^{th} day. CAM assay showed that 5 μg concentration of thyroxine hydrogel not only promoted the invasion of blood vessels but also promoted neovascularization. A thick network of blood vessels was grown in and around the scaffold. 1TA exhibited scaffold attachment with the CAM, but the least blood vessels were attracted toward the scaffold than that of 5TA and 10TA. It could be due to the higher concentration of thyroxine, that is in accordance with the previously published work by our group [37] [53]. The control sample did not show an angiogenic effect. It was concluded that thyroxine promoted angiogenesis. This study proved that 5μg thyroxine is the most suitable amount for angiogenesis; 5TA among all samples has the highest potential to support the blood vessel formation [54].

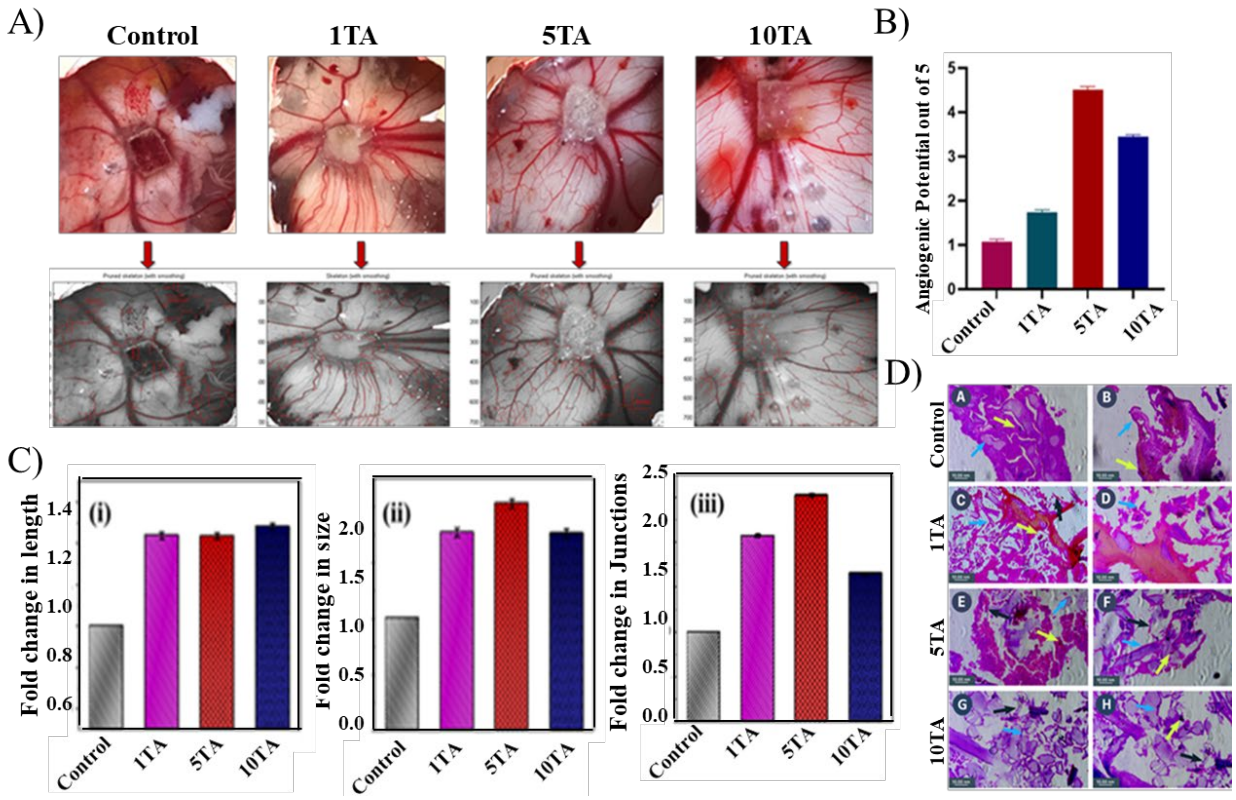

Figure 5: *In ovo* angiogenesis assay performed by using chick embryo model. Four samples were used: A) shows the qualitative images of chick embryo model after 7 days incubation with control, 1TA, 5TA, and 10TA; B) Angiogenic variables such as i) blood vessels length, ii) size & iii) junctions (branches) were enumerated via AngioQuant analysis software; C) Quantification (Blinded) of blood vessels in scaffolds retrieved from CAM assay: D)Images and hematoxylin-eosin staining of ~~hydrogels~~ alginate dressings retrieved from CAM assay, where, black, blue and yellow arrows show blood vessels, blood vessels attached with scaffold and red blood cells respectively.

For quantification, blind scoring technique was applied, that was counted by 5 volunteers. More blood vessels were sprouted around 5TA, as shown in the graph (Fig. 5B). The clear difference was observed between number of blood vessels nurturing around Control, 1TA, 5TA and 10TA.

It was observed that 5TA showed 1.2 folds change in junctions as compared to Control, 1TA and 10TA, as shown in Figure 5(C) (i, ii, iii). The enhanced junctions were might be due to maturation of the pre-existing blood vessels as compared to Control. Overall, the results confirmed that 5TA stimulated angiogenesis better than other studied groups

3.9 Histological analysis (H & E staining)

Histochemical staining, hematoxylin-eosin (H&E), was used to explore re-epithelialization, in samples retrieved from CAM assay. All groups exhibited disposition of neovascularization and fibroblasts, demonstrating the migration of fibroblast cells, angiogenesis within and around the thyroxine loaded scaffolds, as depicted in Fig. 5(D).

In the H and E stained images, for 5TA, there is a pronounced increase in the number of blood vessels and their consistent coalition with the scaffold as compared to control (without thyroxine), 1TA and 10 TA. However, it could be concluded that 5TA contributed an appropriate environment for fibroblast cells proliferation. So, the results of this analysis were very encouraging, keeping in view the presence of many nuclei (purple-stained). The presence of nuclei confirmed the infiltration of cells from the amniotic membrane within all scaffolds. This also proved the biocompatibility of the developed thyroxine and alginate loaded scaffolds. The presence of erythrocytes (red anucleate cells) also revealed the ability of our scaffolds in the new vessels formation (angiogenesis). 5TA helps in the propagation of blood vessels, leading characteristics towards its application in wound healing.

It is well reported in literature that commercially available alginate dressings have many advantages over chitosan based dressings as these have more biocompatibility due to having porous fibrous structure with smooth surface morphology, slow release of thyroxine, hydrophilic nature with excellent water retention capacity, absorbs excessive exudate, provides the cooling effect, holds the drugs and have non adherence with wound bed [55].

4 Conclusions

The thyroxine (1µg, 5µg and 10µg/mL) loaded alginate dressings were prepared by simply dipping alginate dressings into thyroxine solutions. These dressings showed excellent solution absorption capacity and a high swelling ratio due to their interconnected porosity. On treatment with fibroblast cells (NIH-3T3) up to 7 days, these thyroxine releasing dressings proved to be non-toxic and

significantly stimulated cell proliferation. CAM assay proved that 5µg/mL thyroxine containing alginate dressings highly stimulated angiogenesis, four folds increase in the number of blood vessels was observed as compared to simple clinically used alginate dressings. In gene expression study, thyroxine releasing from dresssings was proved to be a dynamic regulator of angiogenesis, which was controlled by VEGF, IL-10, IL-1B and TNF-α in association with various regulating genes, The molecular gene level investigations suggested that angionesis was found to be dependent on the thyroxine concentration. We believe that thyroxine loaded alginate dressings are promising tool for wound healing applications There are number of companies producing alginate dressings which proves high consumption of alginate dressings Worldwide, its more active thyroxine alginate dressings with improved wound healing potential will increase its clinical use at global level.

Acknowledgment:

The authors extend their appreciation to HEC-NRPU 8762 and HEC-NRPU 7780 for funding this study. Further, the authors (Alap Ali Zahid and Anwarul Hasan) would like to acknowledge the NPRP12S-0310-190276 grant funded by the Qatar National Research Fund (a part of the Qatar Foundation).

References

1. Bale, S., et al., *Skin care.* Science and practice of pressure ulcer management, 2018: p. 111-124.
2. Pazyar, N., et al., *Skin wound healing and phytomedicine: a review.* Skin Pharmacology and Physiology, 2014. **27**(6): p. 303-310.
3. Corcione, S. and F.G. De Rosa, *The optimal duration of treatment for skin and soft tissue infections and acute bacterial skin and skin structure infections.* Current Opinion in Infectious Diseases, 2018. **31**(2): p. 155-162.
4. Rittié, L., *Cellular mechanisms of skin repair in humans and other mammals.* Journal of cell communication and signaling, 2016. **10**: p. 103-120.
5. Rosique, R.G., M.J. Rosique, and J.A. Farina Junior, *Curbing inflammation in skin wound healing: a review.* International journal of inflammation, 2015. **2015**.
6. Yolanda, M.-M., et al., *Adult stem cell therapy in chronic wound healing.* J Stem Cell Res Ther, 2014. **4**(162): p. 2.
7. Sorg, H., et al., *Skin wound healing: an update on the current knowledge and concepts.* European Surgical Research, 2017. **58**(1-2): p. 81-94.

8. Pereira, R.F. and P.J. Bartolo, *Traditional therapies for skin wound healing.* Advances in wound care, 2016. **5**(5): p. 208-229.
9. Zhao, X., et al., *Antibacterial anti-oxidant electroactive injectable hydrogel as self-healing wound dressing with hemostasis and adhesiveness for cutaneous wound healing.* Biomaterials, 2017. **122**: p. 34-47.
10. Kamoun, E.A., E.-R.S. Kenawy, and X. Chen, *A review on polymeric hydrogel membranes for wound dressing applications: PVA-based hydrogel dressings.* Journal of advanced research, 2017. **8**(3): p. 217-233.
11. Kim, H., *Wound dressing materials: The essentials.* Journal of Wound Management and Research, 2018. **14**(2): p. 141-142.
12. Seo, S.Y., et al., *Alginate-based composite sponge containing silver nanoparticles synthesized in situ.* Carbohydrate polymers, 2012. **90**(1): p. 109-115.
13. Yang, J.-S., Y.-J. Xie, and W. He, *Research progress on chemical modification of alginate: A review.* Carbohydrate polymers, 2011. **84**(1): p. 33-39.
14. Ching, S.H., N. Bansal, and B. Bhandari, *Alginate gel particles–A review of production techniques and physical properties.* Critical reviews in food science and nutrition, 2017. **57**(6): p. 1133-1152.
15. Aderibigbe, B.A. and B. Buyana, *Alginate in wound dressings.* Pharmaceutics, 2018. **10**(2): p. 42.
16. Lee, K.Y. and D.J. Mooney, *Alginate: properties and biomedical applications.* Progress in polymer science, 2012. **37**(1): p. 106-126.
17. Rowley, J.A., G. Madlambayan, and D.J. Mooney, *Alginate hydrogels as synthetic extracellular matrix materials.* Biomaterials, 1999. **20**(1): p. 45-53.
18. Dai, M., et al., *Chitosan-alginate sponge: preparation and application in curcumin delivery for dermal wound healing in rat.* BioMed Research International, 2009. **2009**.
19. Öztürk, E., et al., *Preparation and characterization of ciprofloxacin-loaded alginate/chitosan sponge as a wound dressing material.* Journal of applied polymer science, 2006. **101**(3): p. 1602-1609.
20. Augustine, R., et al., *CTGF loaded electrospun dual porous core-shell membrane for diabetic wound healing.* International Journal of Nanomedicine, 2019: p. 8573-8588.
21. Ahmed, R., et al., *Bone marrow mesenchymal stem cells preconditioned with nitric-oxide-releasing chitosan/PVA hydrogel accelerate diabetic wound healing in rabbits.* Biomedical Materials, 2021. **16**(3): p. 035014.
22. Rehman, S.R.u., et al., *Reduced graphene oxide incorporated GelMA hydrogel promotes angiogenesis for wound healing applications.* International journal of nanomedicine, 2019: p. 9603-9617.
23. Augustine, R., et al., *Crosslinking strategies to develop hydrogels for biomedical applications.* Nano Hydrogels: Physico-Chemical Properties and Recent Advances in Structural Designing, 2021: p. 21-57.
24. Augustine, R., et al. *Growth factor releasing core-shell polymeric scaffolds for tissue engineering applications*. in *2019 41st Annual International Conference of the IEEE Engineering in Medicine and Biology Society (EMBC)*. 2019. IEEE.
25. ZAHID, A.A., *FABRICATION OF A NITRIC OXIDE RELEASING CHITOSAN-PVA-SNAP*. 2019, QATAR UNIVERSITY.
26. Brix, K., D. Führer, and H. Biebermann, *Molecules important for thyroid hormone synthesis and action-known facts and future perspectives.* Thyroid research, 2011. **4**: p. 1-6.
27. Zaaber, I., et al., *Plasma VEGF-related polymorphisms are implied in autoimmune thyroid diseases.* Autoimmunity, 2016. **49**(4): p. 229-235.

28. Tomanek, R.J. and T.L. Busch, *Coordinated capillary and myocardial growth in response to thyroxine treatment.* The Anatomical Record: An Official Publication of the American Association of Anatomists, 1998. **251**(1): p. 44-49.
29. Dev, N., J. Sankar, and M. Vinay, *Functions of thyroid hormones.* Thyroid Disorders: Basic Science and Clinical Practice, 2016: p. 11-25.
30. Pennock, G.D., et al., *Cardiac effects of 3, 5-diiodothyropropionic acid, a thyroid hormone analog with inotropic selectivity.* Journal of Pharmacology and Experimental Therapeutics, 1992. **263**: p. 163-163.
31. Davis, F.B., et al., *Proangiogenic action of thyroid hormone is fibroblast growth factor–dependent and is initiated at the cell surface.* Circulation research, 2004. **94**(11): p. 1500-1506.
32. Luidens, M.K., et al., *Thyroid hormone and angiogenesis.* Vascular pharmacology, 2010. **52**(3-4): p. 142-145.
33. Sirakov, M., et al., *Thyroid hormone's action on progenitor/stem cell biology: new challenge for a classic hormone?* Biochimica et Biophysica Acta (BBA)-General Subjects, 2013. **1830**(7): p. 3917-3927.
34. Aleem, A.R., et al., *Thyroxin releasing chitosan/collagen based smart hydrogels to stimulate neovascularization.* Materials & Design, 2017. **133**: p. 416-425.
35. Shahzadi, L., et al., *Thyroxine impregnated chitosan-based dressings stimulate angiogenesis and support fast wounds healing in rats: potential clinical candidates.* 2020. **160**: p. 296-306.
36. Waris, T.S., et al., *Design and development of thyroxine/heparin releasing affordable cotton dressings to treat chronic wounds.* 2022. **16**(5): p. 460-471.
37. Aleem, A.R., et al., *Thyroxin releasing chitosan/collagen based smart hydrogels to stimulate neovascularization.* 2017. **133**: p. 416-425.
38. Shahzadi, L., et al., *Triethyl orthoformate covalently cross-linked chitosan-(poly vinyl) alcohol based biodegradable scaffolds with heparin-binding ability for promoting neovascularisation.* Journal of biomaterials applications, 2016. **31**(4): p. 582-593.
39. Gotoh, T., Y. Nakatani, and S. Sakohara, *Novel synthesis of thermosensitive porous hydrogels.* Journal of Applied Polymer Science, 1998. **69**(5): p. 895-906.
40. Guo, D., et al., *Vascular endothelial growth factor signaling requires glycine to promote angiogenesis.* 2017. **7**(1): p. 1-10.
41. Couper, K.N., D.G. Blount, and E.M.J.T.J.o.I. Riley, *IL-10: the master regulator of immunity to infection.* 2008. **180**(9): p. 5771-5777.
42. Iyer, S.S. and G.J.C.R.i.I. Cheng, *Role of interleukin 10 transcriptional regulation in inflammation and autoimmune disease.* 2012. **32**(1).
43. Shams, F., et al., *Overexpression of VEGF in dermal fibroblast cells accelerates the angiogenesis and wound healing function: in vitro and in vivo studies.* Scientific Reports, 2022. **12**(1): p. 18529.
44. Johnson, K.E. and T.A. Wilgus, *Vascular endothelial growth factor and angiogenesis in the regulation of cutaneous wound repair.* Advances in wound care, 2014. **3**(10): p. 647-661.
45. Shaik-Dasthagirisaheb, Y., et al., *Vascular endothelial growth factor (VEGF), mast cells and inflammation.* International journal of immunopathology and pharmacology, 2013. **26**(2): p. 327-335.
46. Lee, T.-H., et al., *Vascular endothelial growth factor modulates neutrophil transendothelial migration via up-regulation of interleukin-8 in human brain microvascular endothelial cells.* Journal of Biological Chemistry, 2002. **277**(12): p. 10445-10451.
47. Schweighofer, B., et al., *The VEGF-induced transcriptional response comprises gene clusters at the crossroad of angiogenesis and inflammation.* Thrombosis and haemostasis, 2009. **102**(09): p. 544-554.

48. Maloney, J.P. and L. Gao, *Proinflammatory cytokines increase vascular endothelial growth factor expression in alveolar epithelial cells.* Mediators of inflammation, 2015. **2015**.
49. Reinders, M.E., et al., *Proinflammatory functions of vascular endothelial growth factor in alloimmunity.* The Journal of clinical investigation, 2003. **112**(11): p. 1655-1665.
50. Morrissey, P.J. and D.Y. Mochizuki, *Interleukin-1 is identical to hemopoietin-1: studies on its therapeutic effects on myelopoiesis and lymphopoiesis.* Biotherapy, 1989. **1**(4): p. 281-291.
51. Fahey, E. and S.L. Doyle, *IL-1 family cytokine regulation of vascular permeability and angiogenesis.* Frontiers in Immunology, 2019. **10**: p. 1426.
52. Mohr, T., et al., *Proteome profiling in IL-1β and VEGF-activated human umbilical vein endothelial cells delineates the interlink between inflammation and angiogenesis.* PloS one, 2017. **12**(6): p. e0179065.
53. Malik, M.H., et al., *Thyroxine-loaded chitosan/carboxymethyl cellulose/hydroxyapatite hydrogels enhance angiogenesis in in-ovo experiments.* 2020. **145**: p. 1162-1170.
54. Zubairi, W., et al., *Evaluation of angiogenic potential of heparin and thyroxine releasing wound dressings.* 2021: p. 1-12.
55. Barbu, A., et al., *Current trends in advanced alginate-based wound dressings for chronic wounds.* Journal of Personalized Medicine, 2021. **11**(9): p. 890.